Journal of Applied Physics ARTICLE scitation.org/journal/jap

Coupled spin waves and crystalline electric field levels in candidate multiferroic $ErFeO_3$

Cite as: J. Appl. Phys. **130**, 014102 (2021); doi: 10.1063/5.0054226
Submitted: 15 April 2021 · Accepted: 9 June 2021 ·
Published Online: 6 July 2021

View Online Export Citation CrossMark

Mark P. Zic,[1,2] Wesley T. Fuhrman,[1,2] Kefeng Wang,[2] Sheng Ran,[1,2] Johnpierre Paglione,[2,3] and Nicholas P. Butch[1,2,a)]

AFFILIATIONS

[1]NIST Center for Neutron Research, National Institute of Standards and Technology, Gaithersburg, Maryland 20899, USA
[2]Maryland Quantum Materials Center, Department of Physics, University of Maryland, College Park, Maryland 20742, USA
[3]Canadian Institute for Advanced Research, Toronto, Ontario M5G 1Z8, Canada

[a)]**Author to whom correspondence should be addressed:** nbutch@umd.edu

ABSTRACT

We report an inelastic neutron scattering study of candidate multiferroic $ErFeO_3$, a compound that has been previously reported to have three different magnetic states and undergoes signatures of Fe^{3+}–Er^{3+} cooperative coupling. The spectrum at low energy transfer is dominated by excitations of the Er^{3+} character, even above the Er^{3+} antiferromagnetic ordering temperature of 4.5 K. In addition, a crystalline electric field excitation at 6 meV exhibits additional energy splitting upon cooling through 4.5 K with mode-dependent polarization. This indicates different moment directions for these modes, an interesting consequence of C_y ordering of the Er^{3+} moments.

I. INTRODUCTION

Multiferroic materials are materials in which ferroelectricity coexists with magnetic order,[1] possessing possible applications in magnetic field sensors, spin valves, spin filters, and memory devices.[2] Multiferroicity has been found in many different compounds in the ABO_3 ($A \equiv 4f$ rare earth, $B \equiv 3d$ transition metal) family,[3–5] originating from inversion breaking magnetic states.[6]

$ErFeO_3$ belongs to the $AFeO_3$ subset of the larger ABO_3 family. Members of this class of materials such as $SmFeO_3$,[7,8] $DyFeO_3$,[9,10] and $GdFeO_3$,[11] exhibit peculiar phenomena such as room temperature multiferrocity,[7] large magnetoelectric coupling,[9] and giant reversible magnetocaloric effect,[11] respectively.

A high Néel temperature makes $ErFeO_3$ useful in understanding the physics of room-temperature multiferroic materials. $ErFeO_3$ undergoes three different magnetic transitions on two different magnetic sublattices,[12] one being a spin-reorientation transition that becomes discontinuous at high magnetic fields.[13] Below 4.5 K, the Er^{3+} sublattice orders with an antiferromagnetic structure and the canted magnetic structure of the Fe^{3+} sublattice changes slightly [Figs. 1(a) and 1(b)]. The temperature ranges in which the phases exist and corresponding magnetic structures are (in terms of the Pnma structure) (a) $T < 4.5$ K, Er^{3+}: C_y and Fe^{3+}: $C_xG_yF_z$ and (b) 4.5 K $< T <$ 110 K, Fe^{3+}: G_yF_z; (unpictured) 110 K $< T <$ 650 K, Fe^{3+}: F_yG_z. In Figs. 1(a) and 1(b), red balls and arrows denote Er^{3+} atoms and moments, respectively; cyan balls and arrows denote Fe^{3+} atoms and moments, respectively. O sites are omitted for clarity. The canting angle of the iron moments in the low-temperature range is reported to be about 45°, while that of the 4.5 K $< T <$ 110 K range is nearly zero.[14] Figures 1(a) and 1(b) are drawn using a Pbnm unit cell.

This has potential for interesting physics because both magnetic Fe^{3+} and Er^{3+} ionic sublattices are ordered with different structures and energy scales, allowing for complex interactions between these ions. Some low-temperature interactions were revealed by a study on Y-doped $ErFeO_3$ samples, in a magnetic field, using optical spectroscopy to observe Dicke cooperativity.[15] Previous inelastic neutron scattering has shown that $ErFeO_3$ possesses low energy, $\mathbf{Q} = 0$ magnons down to 70 K.[16] In addition, optical spectroscopy measurements[17–19] have identified local splittings at 0.8, 5.7, 6.2, 14.0, and 20.6 meV. However, there has been no report of the dispersions of low-energy magnetic excitations below the Er^{3+} ordering temperature in this material.

Our low-temperature inelastic neutron scattering study corroborates previous spectroscopic studies, identifies the momentum-dependence of the magnetic spectra, and uncovers yet

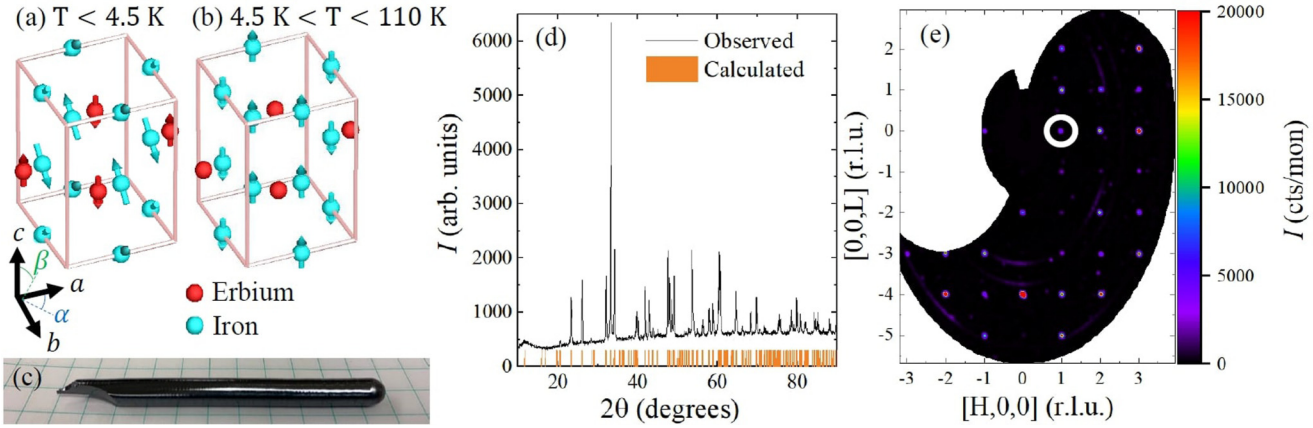

FIG. 1. (a) and (b) $ErFeO_3$ undergoes three magnetic transitions.[12] The two lower temperature phases are plotted here using ISODISTORT[22] in the Pbnm crystal structure. The angles α and β are defined later in Sec. IV and are shown here for clarity. (c) The single crystal used for our measurements atop a sheet of 1×1 cm^2 grid paper. (d) Powder x-ray diffraction done on our single crystal of $ErFeO_3$; all peaks were identified to be those of $ErFeO_3$. (e) Elastic scattering in the [H,0,L] plane at 1.5 K with energy averaged over [−0.1,0.1] meV. Sharp peaks at integer [H,0,L] demonstrate good crystallinity. Notice the magnetic peak that breaks lattice symmetry at [1,0,0] (circled) due to the ordering of the erbium sites, which is not present above 4.5 K.

another interesting facet of multiferroics: the collective excitations of robust crystal field modes and spin waves. Comparison of the magnetic excitations above and below the erbium ordering transition highlights the importance of both spin–spin interactions and spin anisotropy in this system.

II. EXPERIMENTAL METHODS

A rod-shaped crystal of $ErFeO_3$ was grown [Fig. 1(d)] using the method described by Koohpayeh *et al.*[20] with a growth rate of 3 mm/h. A small piece of this single crystal was analyzed via powder x-ray diffraction [Fig. 1(c)] to confirm that it formed in the orthorombic Pbnm pseudo-cubic perovskite structure with lattice parameters $a = 5.262$ Å, $b = 5.583$ Å, and $c = 7.593$ Å.[21] Note that $ErFeO_3$ is often reported with Pnma crystal structure with $a' = b$, $b' = c$, and $c' = a$, where the primed variables are the lattice constants of the Pnma structure.

The crystal was cut width-wise into three roughly equal rods of a total mass of 14.5 g. X-ray Laue diffraction measurements indicated that the $ErFeO_3$ rods had good crystallinity. The $ErFeO_3$ rods were co-aligned in the crystallographic *ac*-plane ([H,0,L] scattering plane), with the crystalline *c*-axis oriented along the long axis of the rod.

For the inelastic neutron scattering measurements, we utilized the Disk Chopper Spectrometer (DCS) at the National Institute for Standards and Technology (NIST) Center for Neutron Research (NCNR).[23] Measurements were performed in three configurations: (1) incident wavelength 1.8 Å (24 meV) with an energy resolution of 2 meV full-width at half maximum at elastic energy transfer, (2) incident wavelength 2.5 Å (12 meV) with an energy resolution of 0.4 meV full-width at half maximum at elastic energy transfer, and (3) incident wavelength 5 Å (3 meV) with an energy resolution of 0.1 meV full-width at half maximum at elastic energy transfer. Scans of these wavelengths were conducted at 6 and 1.5 K, above and below the Er^{3+} sublattice ordering temperature,[12] to examine the spectra in great detail. Data analysis was done using the DAVE software from the NIST Center for Neutron Research.[24] Time-independent background was estimated from low-temperature negative energy transfer data. Absolute units were obtained by measuring the incoherent scattering away from magnetic and structural Bragg peaks at 5 Å and then scaling the short wavelength data.[25,26] We normalized the scattered intensity to determine the fluctuating magnetic moment per site times the form factor squared,

$$M'(\mathbf{Q},\omega) = \widetilde{M}(\mathbf{Q},\omega)|f(\mathbf{Q})|^2 \quad (1)$$

in units of $\mu_B^2\,\mathrm{meV}^{-1}$, where $\mathbf{Q}$ is the momentum transfer and ω is the energy transfer.

III. EXPERIMENTAL RESULTS

Elastic scattering shows good crystallinity in our single crystals with peaks at integer [H,0,L] [Fig. 1(e)], including a lattice symmetry breaking Bragg peak at [H,K,L] = [1,0,0] that is due to the ordering of the erbium sublattice below 4.5 K.

Characteristic of Fe-based multiferroics, energetic Fe^{3+} modes are present at odd [H,0,L] at a base temperature of 1.5 K. The dispersion of these waves is very sharp and has a bandgap of approximately 9 meV [Fig. 2(a)]. Short wavelength measurements also have revealed a **Q**-independent mode at 14 meV and a very low intensity mode at about 21 meV [Fig. 2(b)]. The peak width of the 14 and 21 meV modes are instrument resolution limited, which has a value of 1.3 meV full-width at half maximum here. The 14 meV and 21 meV excitations closely match those previously measured via optical spectroscopy on $ErFeO_3$.[18]

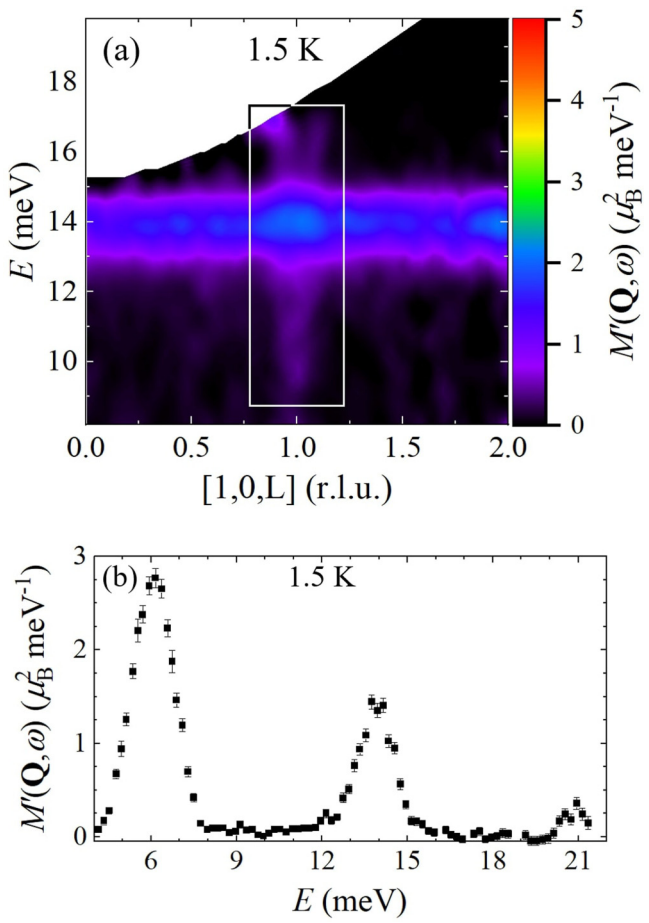

FIG. 2. Survey of excitations in $ErFeO_3$ at 1.5 K. (a) Dispersion of the sharply dispersing Fe^{3+} spin waves along [1,0,L] with a bandgap of approximately 9 meV, boxed for emphasis. This signature is periodic at odd values of H and L. (b) These coexist with Er^{3+}-derived flat modes at 6, 14, and 21 meV. The window of momentum averaging for this plot is [2,6] (r.l.u.) in H and [0.9,1.1] (r.l.u.) in L. The uncertainties in this figure correspond to one standard deviation.

At low energies, we observe a dispersive mode at 0.4 meV at 6 K [Figs. 3(a) and 3(b)]. The anisotropic **Q**-space modulation can be accounted for by a polarization factor with moments along the *c*-axis [Fig. 4(a)]. This polarization factor is defined as the term p_i (i = H, K, L),[27]

$$p_i = 1 - \frac{Q_i^2}{Q_H^2 + Q_K^2 + Q_L^2}. \tag{2}$$

In this notation, Q_i is the crystal momentum along the i direction. This modifies the intensity of the spin waves observed via

$$\int I(\mathbf{Q}, E)dE \propto |f(\mathbf{Q})|^2 \cdot p_i, \tag{3}$$

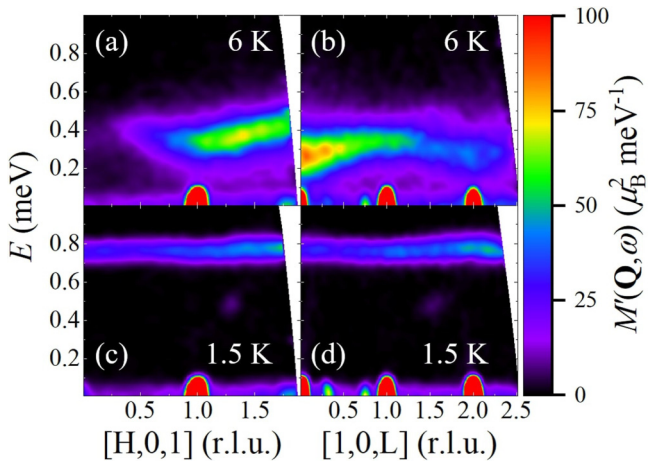

FIG. 3. Dispersion (a) and (b) above (6 K) and (c) and (d) below (1.5 K) the ordering temperature of the Er^{3+} moments along (a) and (c) [H,0,1] and (b) and (d) [1,0,L]. At 6 K, we observe a low energy magnon at 0.4 meV with a peak-to-peak width of about 0.1 meV originating from the splitting of the ground state doublet.[19] At 1.5 K, this excitation shifts to about 0.8 meV and becomes much less dispersive with a peak-to-peak width of approximately 0.02 meV. The higher temperature mode is polarized along L (Fig. 4), whereas the 1.5 K mode is unpolarized. For all spectra, the window of averaging is [0.9,1.1] reciprocal lattice units in the perpendicular direction.

where the left-hand side is the intensity observed as a function of energy and crystal momentum, which is proportional to the magnetic ion form factor ($|f(\mathbf{Q})|$) and the spin-polarization factor. The polarization of the 0.4 meV mode is consistent with moments along c [as shown in Fig. 4(b)], since the strongest intensity will be shown for **Q** perpendicular to the moment direction.

When cooled to 1.5 K, this mode increases in energy to about 0.8 meV with a decreased dispersion [Figs. 3(c) and 3(d)] and no longer appears to be polarized. This mode softening with increased temperature matches the temperature dependence of the splitting of the Er^{3+} ground state Kramers doublet determined previously in

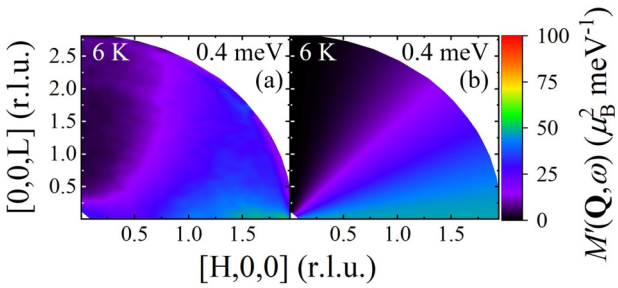

FIG. 4. (a) Polarization of the 0.4 meV mode at 6 K, demonstrating the polarization of the spins along the *c*-axis. The window of averaging of the mode is [0.1,0.6] meV. (b) The mode is consistent with moments completely along the *c*-axis, as modeled by Eq. (2).

optical measurements.[19] The splitting was attributed to dipolar fields arising from displacements of the erbium atoms from ideal high-symmetry positions, the effects of which persist to at least 77 K. Our results at 6 K show appreciable dispersion, consistent with the paramagnetic erbium moments being influenced by an effective internal field created by the ordered iron moments at these temperatures.

At 5.7 meV, a mode that is only dispersive along [0,0,L] is present at 6 K [Figs. 5(a) and 5(c)]. This mode shifts and splits upon cooling to 1.5 K, below the Er^{3+} antiferromagnetic ordering temperature of 4.5 K [Figs. 5(b) and 5(d)]. The dispersion solely along the [0,0,L] direction persists in the low-temperature state. These split modes have approximate energies 6.3 and 5.8 meV at 1.5 K. These excitations are consistent with previous assignments of erbium crystal electric field (CEF) levels,[17–19] but the dispersion along [0,0,L] indicates that there are appreciable erbium interactions along the *c* direction.

The excitations at 1.5 K have similar intensity along the [H,0,0] direction but have drastically different intensities along the [0,0,L] direction. This is consistent with the polarization factor of these modes [Figs. 6(a) and 6(b)]. Note that the 5.8 meV dispersion has a spin-polarization factor along [0,0,L], while the CEF at 6.3 meV has a spin-polarization factor along [H,0,0]. The polarization of these two excitations is clearly different from the static magnetic structure with moments purely along *c*.

IV. DISCUSSION

The magnetic interactions are complicated in $ErFeO_3$, owing to canted moments on the Fe^{3+} sublattice as well as two magnetic species. In addition to this, the crystal electric field-split states can have different magnetization densities and moment directions, making an even more complex system.

With regard to the dispersive CEF modes as presented in Fig. 5, there are a few perplexing qualities. Though the excitation is on the energy scale of $T_{N,Er^{3+}}$ (4.5 K ≈ 0.39 meV), the dispersive CEF modes are present above and below the ordering temperature of the Er^{3+} moments. This could indicate appreciable coupling between the Er^{3+} and Fe^{3+} moments above $T_{N,Er^{3+}}$. Another possible origin of this mode could be from paramagnetic Er^{3+} moments polarized by the Fe^{3+} sublattice. Regardless, it is worthy to note that these modes remain robust through $T_{N,Er^{3+}}$, indicating that the Hamiltonian describing this excitation changes little after the ordering of the Er^{3+} moments. However, this does not necessarily

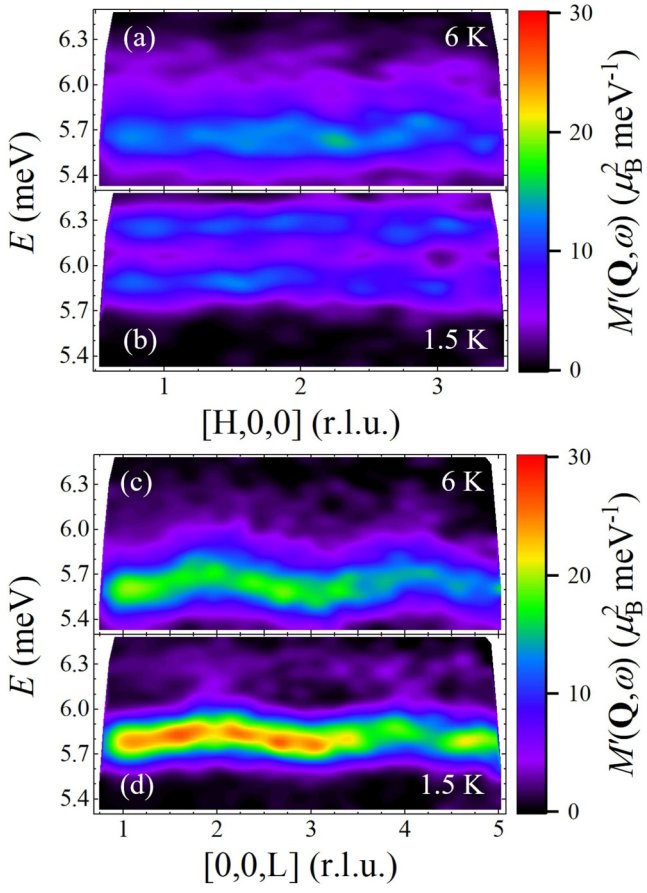

FIG. 5. Splitting of the 5.7 meV crystal field level in $ErFeO_3$. Spectra taken at (a) and (c) 6 K and (b) and (d) 1.5 K. (a) and (b) are averaged over [−0.1,0.1] in L, whereas (c) and (d) are averaged over [−0.1,0.1] in H. Along the [H,0,0] direction (a) and (b), a flat mode splits into two bands upon cooling. Along the [0,0,L] direction, we observe that these bands have dispersion, and that the bottom mode (5.8 meV) has much greater intensity along this direction compared to the top mode (6.3 meV). This is a result of a polarization factor, as seen in Fig. 6.

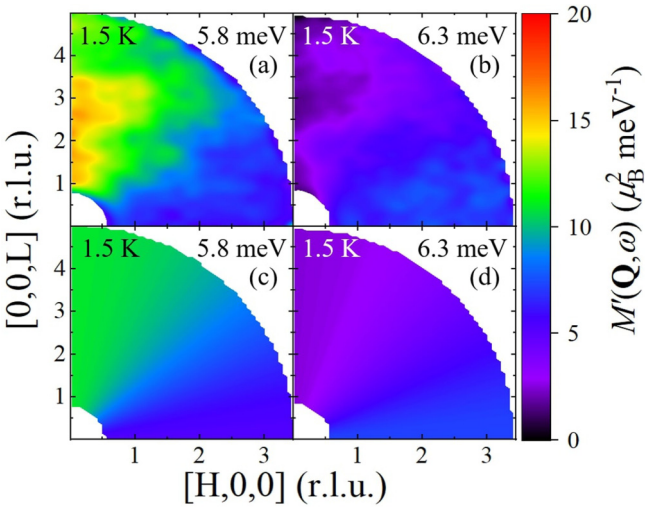

FIG. 6. Base temperature (1.5 K) constant energy cuts at (a) 5.8 meV and (b) 6.3 meV, with windows of averaging of [5.6,6] and [6.1,6.5] meV, respectively. Polarization for the lower energy mode in (a) is along [0,0,L], while that for the higher energy mode in (b) is along [H,0,0]. Figures (c) and (d) display simulated data [modeled by Eqs. (4) and (5), respectively], which well describe the polarization shown in (a) and (b), respectively.

indicate that the coupling between the Er^{3+} and Fe^{3+} moments is small. In $YbFeO_3$,[27] the introduction of J_{Yb-Fe} does not change the excitations, though its value, which is related to the Fe spin-reorientation transition temperature, is higher than that of J_{Yb-Yb}, which does produce collective excitations and hence changes the spectra at low energies in $YbFeO_3$. We believe the case is similar to $ErFeO_3$. Further splitting of these modes, as well as the distinctly different moment directions (as indicated by the different polarizations in Fig. 6), presents further challenges in understanding the physical origin of the dispersive CEF modes, which must be explored further.

As for the polarization data, we can extract values of the polarization factor for the 5.8 and 6.3 meV modes seen at 1.5 K. For this analysis, we assume that the moments lie out of the *ac* plane due to possible interactions with the Fe^{3+} moments, which have their moment partially along *b*. We fit the data of the 5.8 meV mode to

$$p_{\mathrm{H0L},\alpha} = C_\alpha \frac{\sin^2\alpha Q_H^2 + Q_L^2}{Q_H^2 + Q_L^2}, \tag{4}$$

where C_α is a scaling factor and α is the angle of the moments away from *a* in the *ab* plane. Similarly, we fit the data of the 6.3 meV mode to

$$p_{\mathrm{H0L},\beta} = C_\beta \frac{Q_H^2 + \sin^2\beta Q_L^2}{Q_H^2 + Q_L^2}, \tag{5}$$

where C_β is a scaling factor and β is the angle of the moments away from *c* in the *bc* plane. The angles α and β are shown in Figs. 1(a) and 1(b) for clarity.

The best fit was acquired for the two datasets with the following moment angles: $\alpha = 44.21 \pm 0.43^\circ$ and $\beta = 35.88 \pm 0.25^\circ$. The moment directions of these modes are clearly very different than the ground state magnetic structure, with polarization far away from the *c*-axis. A more precise determination of this possible canting in the *ac* plane would require further measurements in a different scattering geometry.

With regard to the 6 K mode at 0.4 meV, it is interesting to note that the scale of the interactions, as identified by the bandwidth, is on the order of the erbium sublattice ordering temperature. This, along with the polarization of the spins along *c*, indicates that appreciable interactions are present above the erbium sublattice ordering temperature. Indeed, the polarization of this low energy mode suggests that the moments are in the same direction as described previously.[12]

Our discovery that CEF-like excitations exhibit appreciable temperature-dependent dispersion suggests that it would be very informative to perform further inelastic neutron scattering studies at higher energy transfer to fully investigate the complicated Er–Fe interactions at low temperatures. We also expect that an applied magnetic field will strongly influence the magnetic moment polarization of the low-energy excitations.

V. SUMMARY AND CONCLUSION

We performed inelastic neutron scattering measurements on $ErFeO_3$ and found that our measurements agree well with the energy levels observed in earlier optical spectroscopic measurements. Although they resemble CEF modes, some of these excitations are dispersive, indicating collective behavior. The higher temperature dispersion is consistent with Fe^{3+}–Er^{3+} magnetic coupling, while Er^{3+} spin waves develop below the Er^{3+} sublattice ordering temperature of 4.5 K. We also presented how the intensity of these excitations varying in the [H,0,L] plane provides evidence for spin canting.

Because of the interplay of spin waves and crystal fields, we emphasize that future work needs to be done on $ErFeO_3$ and others in the $AFeO_3$ family of compounds. Optical and neutron spectroscopy, especially in a field, may elucidate more novel phenomena in these materials.

ACKNOWLEDGMENTS

The authors would like to thank helpful discussions with Brandon Wilfong, Richard L. Greene, Jonathan Gaudet, and Paul M. Neves. Support for M.P.Z. was provided by the Center for High Resolution Neutron Scattering, a partnership between the National Institute of Standards and Technology and the National Science Foundation under Agreement No. DMR-1508249. M.P.Z. also acknowledges support for undergraduate research from the Maryland Quantum Materials Center. W.T.F. is grateful to the Schmidt Science Fellows program, in partnership with the Rhodes Trust, for the partial support of this work. Materials synthesis at UMD was supported by Gordon and Betty Moore Foundation's EPiQS Initiative through Grant No. GBMF9071 and the NIST Center for Neutron Research.

DATA AVAILABILITY

The data that support the findings of this study are available from the corresponding author upon reasonable request.

REFERENCES

[1]M. Fiebig, T. Lottermoser, D. Meier, and M. Trassin, "The evolution of multiferroics," Nat. Rev. Mater. **1**, 16046 (2016).
[2]K. Wang, J.-M. Liu, and Z. Ren, "Multiferroicity: The coupling between magnetic and polarization orders," Adv. Phys. **58**, 321–448 (2009).
[3]M. Fiebig, "Revival of the magnetoelectric effect," J. Phys. D: Appl. Phys. **38**, R123–R152 (2005).
[4]D. Khomskii, "Multiferroics: Different ways to combine magnetism and ferroelectricity," J. Magn. Magn. Mater. **306**, 1–8 (2006).
[5]W. Eerenstein, N. D. Mathur, and J. F. Scott, "Multiferroic and magnetoelectric materials," Nature **442**, 759–765 (2006).
[6]R. E. Cohen, "Origin of ferroelectricity in perovskite oxides," Nature **358**, 136–138 (1992).
[7]J.-H. Lee, Y. K. Jeong, J. H. Park, M.-A. Oak, H. M. Jang, J. Y. Son, and J. F. Scott, "Spin-canting-induced improper ferroelectricity and spontaneous magnetization reversal in $SmFeO_3$," Phys. Rev. Lett. **107**, 117201 (2011).
[8]C.-Y. Kuo, Y. Drees, M. T. Fernández-Díaz, L. Zhao, L. Vasylechko, D. Sheptyakov, A. M. T. Bell, T. W. Pi, H.-J. Lin, M.-K. Wu, E. Pellegrin, S. M. Valvidares, Z. W. Li, P. Adler, A. Todorova, R. Küchler, A. Steppke, L. H. Tjeng, Z. Hu, and A. C. Komarek, "$k = 0$ Magnetic structure and absence of ferroelectricity in $SmFeO_3$," Phys. Rev. Lett. **113**, 217203 (2014).
[9]Y. Tokunaga, S. Iguchi, T. Arima, and Y. Tokura, "Magnetic-field-induced ferroelectric state in $DyFeO_3$," Phys. Rev. Lett. **101**, 097205 (2008).

[10]L. A. Prelorendjo, C. E. Johnson, M. F. Thomas, and B. M. Wanklyn, "Spin reorientation transitions in $DyFeO_3$ induced by magnetic fields," J. Phys. C: Solid State Phys. **13**, 2567–2578 (1980).
[11]M. Das, S. Roy, and P. Mandal, "Giant reversible magnetocaloric effect in a multiferroic $GdFeO_3$ single crystal," Phys. Rev. B **96**, 174405 (2017).
[12]G. Deng, P. Guo, W. Ren, S. Cao, H. E. Maynard-Casely, M. Avdeev, and G. J. McIntyre, "The magnetic structures and transitions of a potential multiferroic orthoferrite $ErFeO_3$," J. Appl. Phys. **117**, 164105 (2015).
[13]H. Shen, Z. Cheng, F. Hong, J. Xu, S. Yuan, S. Cao, and X. Wang, "Magnetic field induced discontinuous spin reorientation in $ErFeO_3$ single crystal," Appl. Phys. Lett. **103**, 192404 (2013).
[14]V. Khmara, N. Kovtun, and G. Troitskii, "Spin configuration of $ErFeO_3$ below the ordering temperature of erbium," Solid State Commun. **15**, 1769–1771 (1974).
[15]X. Li, M. Bamba, N. Yuan, Q. Zhang, Y. Zhao, M. Xiang, K. Xu, Z. Jin, W. Ren, G. Ma, S. Cao, D. Turchinovich, and J. Kono, "Observation of Dicke cooperativity in magnetic interactions," Science **361**, 794–797 (2018).
[16]S. M. Shapiro, J. D. Axe, and J. P. Remeika, "Neutron-scattering studies of spin waves in rare-earth orthoferrites," Phys. Rev. B **10**, 2014–2021 (1974).
[17]R. V. Mikhaylovskiy, T. J. Huisman, R. V. Pisarev, T. Rasing, and A. V. Kimel, "Selective excitation of terahertz magnetic and electric dipoles in Er^{3+} ions by femtosecond laser pulses in $ErFeO_3$," Phys. Rev. Lett. **118**, 017205 (2017).
[18]D. L. Wood, L. M. Holmes, and J. P. Remeika, "Exchange fields and optical Zeeman effect in $ErFeO_3$," Phys. Rev. **185**, 689–695 (1969).
[19]R. Faulhaber, S. Hüfner, E. Orlich, and H. Schuchert, "Optical investigation of $ErFeO_3$," Z. Phys. **204**, 101–113 (1967).
[20]S. Koohpayeh, J. Abell, K. Bamzai, A. Bevan, D. Fort, and A. Williams, "The influence of growth rate on the microstructural and magnetic properties of float-zone grown $ErFeO_3$ crystals," J. Magn. Magn. Mater. **309**, 119–125 (2007).
[21]A. Bombik, B. Leśniewska, J. Mayer, and A. W. Pacyna, "Crystal structure of solid solutions $REFe_{1-x}(Al \text{ or } Ga)_xO_3$ (RE = Tb, Er, Tm) and the correlation between superexchange interaction $Fe^{+3}-O^{-2}-Fe^{+3}$ linkage angles and Néel temperature," J. Magn. Magn. Mater. **257**, 206–219 (2003).
[22]B. J. Campbell, H. T. Stokes, D. E. Tanner, and D. M. Hatch, "Isodisplace: A web-based tool for exploring structural distortions," J. Appl. Crystallogr. **39**, 607–614 (2016).
[23]J. Copley and J. Cook, "The disk chopper spectrometer at NIST: A new instrument for quasielastic neutron scattering studies," Chem. Phys. **292**, 477–485 (2003).
[24]R. T. Azuah, L. R. Kneller, Y. Qiu, P. L. W. Tregenna-Piggott, C. M. Brown, J. R. D. Copley, and R. M. Dimeo, "DAVE: A comprehensive software suite for the reduction, visualization, and analysis of low energy neutron spectroscopic data," J. Res. Natl. Inst. Stand. Technol. **114**, 341–358 (2009).
[25]G. Xu, Z. Xu, and J. M. Tranquada, "Absolute cross-section normalization of magnetic neutron scattering data," Rev. Sci. Instrum. **84**, 083906 (2013).
[26]V. F. Sears, "Neutron scattering lengths and cross sections," Neutron News **3**, 26–37 (1992).
[27]S. E. Nikitin, L. S. Wu, A. S. Sefat, K. A. Shaykhutdinov, Z. Lu, S. Meng, E. V. Pomjakushina, K. Conder, G. Ehlers, M. D. Lumsden, A. I. Kolesnikov, S. Barilo, S. A. Guretskii, D. S. Inosov, and A. Podlesnyak, "Decoupled spin dynamics in the rare-earth orthoferrite $YbFeO_3$: Evolution of magnetic excitations through the spin-reorientation transition," Phys. Rev. B **98**, 064424 (2018).